Carcinogenesis vol.29 no.6 pp.1124–1133, 2008
doi:10.1093/carcin/bgn093
Advance Access publication April 15, 2008

Bioenergetic differences selectively sensitize tumorigenic liver progenitor cells to a new gold(I) compound

Matthew M.Jellicoe[1,2], Scott J.Nichols[1], Bernard A.Callus[3], Murray V.Baker[4], Peter J.Barnard[4], Susan J.Berners-Price[4], James Whelan[5], George C.Yeoh[1,2] and Aleksandra Filipovska[1,2,*]

[1]Laboratory for Cancer Medicine, Western Australian Institute for Medical Research and Center for Medical Research, The University of Western Australia, Perth, Western Australia 6000, Australia, [2]Biochemistry, School of Biomedical, Biomolecular and Chemical Sciences, The University of Western Australia, 35 Stirling Highway, Crawley, Western Australia 6009, Australia, [3]Department of Biochemistry, La Trobe University, Victoria 3086, Australia, [4]Chemistry, School of Biomedical, Biomolecular and Chemical Sciences, The University of Western Australia, 35 Stirling Highway, Crawley, Western Australia 6009, Australia and [5]Australian Research Council Centre of Excellence in Plant Energy Biology, The University of Western Australia, Western Australia 6009, Australia

[*]To whom correspondence should be addressed. Tel: +61 8 9224 0330; Fax: +61 8 9224 0322;
Email: afilipov@waimr.uwa.edu.au

A hallmark of cancer cells is their ability to evade apoptosis and mitochondria play a critical role in this process. Delineating mitochondrial differences between normal and cancer cells has proven challenging due to the lack of matched cell lines. Here, we compare two matched liver progenitor cell (LPC) lines, one non-tumorigenic [p53-immortalized liver (PIL) 4] and the other tumorigenic (PIL2). Analysis of these cell lines and a p53 wild-type non-tumorigenic cell line [bipotential murine oval liver (BMOL)] revealed an increase in expression of genes encoding the antiapoptotic proteins cellular inhibitor of apoptosis protein (cIAP) 1 and yes associate protein in the PIL2 cells, which resulted in an increase in the protein encoded by these genes. PIL2 cells have higher mitochondrial membrane potential ($\Delta\psi_m$) compared with PIL4 and BMOL and had greater levels of reactive oxygen species, despite the fact that the mitochondrial antioxidant enzyme, manganese superoxide disumutase, was elevated at transcript and protein levels. Taken together, these results may account for the observed resistance of PIL2 cells to apoptotic stimuli compared with PIL4. We tested a new gold compound to show that hyperpolarized $\Delta\psi_m$ led to its increased accumulation in mitochondria of PIL2 cells. This compound selectively induces apoptosis in PIL2 cells but not in PIL4 or BMOL. The gold compound depolarized the $\Delta\psi_m$, depleted the adenosine triphosphate pool and activated caspase-3 and caspase-9, suggesting that apoptosis was mediated via mitochondria. This investigation shows that the non-tumorigenic and tumorigenic LPCs are useful models to delineate the role of mitochondrial dysfunction in tumorigenesis and for the future development of mitochondria-targeted chemotherapeutics that selectively target tumor cells.

Introduction

Liver progenitor cells (LPCs) are observed in liver pathologies such as genetic hemochromatosis, viral hepatitis (Hepatitis B Virus and Hepatitis C Virus) and in chronic alcoholic liver disease (1,2), all conditions that are associated with an increased incidence of hepatocellular carcinoma (HCC). Animal studies have shown that LPC can convert to HCC by forced expression of c-myc and ras (3) and we have shown that incidence of HCC correlates with LPC numbers in tumor necrosis factor receptor knockout mice (4). There is evidence that mitochondrial dysfunction plays a key role in liver disease and HCC (5,6). HCC cells have reduced oxidative phosphorylation and decreased activity of cytochrome c oxidase, ATPase and the adenine nucleotide translocator (6–10). Although these studies indicate that LPCs can be targets for transformation, the changes responsible for their alteration to cancer and specifically the role of mitochondrial function remain elusive. Genomic and proteomic profiling of the molecular differences between non-tumorigenic and tumorigenic cells have been challenging because of the lack of appropriately matched cell lines. In this study, we have exploited two LPC lines, one non-tumorigenic [p53-immortalized liver (PIL) 4] and the other tumorigenic (PIL2) established from the same strain of mice, by the same protocol to reveal differences in the expression of genes involved in apoptosis and mitochondrial function. The identified differences between non-tumorigenic and tumorigenic LPCs can be exploited to develop chemotherapeutics with selective antitumor activity.

Mitochondria play a central role in energy production. The transport of electrons from reducing equivalents through the mitochondrial respiratory complexes is coupled to proton pumping out of the mitochondrial matrix that generates a high electrochemical gradient across the mitochondrial inner membrane used to produce adenosine triphosphate (ATP). The electrical component of the gradient, mitochondrial membrane potential ($\Delta\psi_m$), can differ between cell states and cell types. A survey of >200 different cell types showed that carcinomas have up to a 60 mV increase in $\Delta\psi_m$ compared with normal epithelial cells (11–13). Recently, suggestions that $\Delta\psi_m$ changes may reflect tumor progression are supported by findings that subpopulations of a colonic carcinoma cell line with a higher $\Delta\psi_m$ are more tumorigenic (14). This raises the possibility that tumor progression may be associated with changes in $\Delta\psi_m$ and furthermore that this increase may be responsible for their evasion of apoptosis and resistance to chemotherapeutics. In addition, increased expression of antiapoptotic proteins (such as Bcl-2 and Bcl-X_L) and loss of proapoptotic proteins (such as Bax) have been identified in many cancers as the cause for the cells' resistance to apoptotic stimuli and decreased response to chemotherapy (15–18).

The origin and consequence of the elevated $\Delta\psi_m$ in cancer cells is unknown, although it has been exploited as a potential target for their destruction. Delocalized lipophilic cations (DLCs) can pass easily through the lipid bilayer and their positive charge then directs them to the mitochondria where they accumulate at significantly higher concentrations than in the cytoplasm because of the large $\Delta\psi_m$ (19). DLCs have been explored as a new approach to cancer chemotherapy by exploiting their selective accumulation in mitochondria of cancer cells as a consequence of their elevated $\Delta\psi_m$. The structures of DLCs are diverse and consequently their mechanism of action and mitochondrial targets vary (20). Some lipophilic, cationic gold(I) phosphine compounds have shown early promise as anticancer drugs (21); although their mechanism of cytotoxicity is still unclear, their behavior is consistent with that of other DLCs, which exhibit antitumor activity (22). Previous studies have shown that by fine-tuning the hydrophilic–lipophilic balance, it is possible to synthesize gold(I) compounds that are able to target mitochondria with great specificity (23). Recently, we have shown a remarkable selective toxicity of a gold(I) complex for cancer cells as a result of their increased $\Delta\psi_m$ (24). While these DLCs promised benefit may arise from targeting the elevated $\Delta\psi_m$ of cancer cells, there needs to be a systematic study that includes a comparison of a non-transformed cell and its direct transformed counterpart of the same lineage. The response of both cell types needs to be evaluated, as they coexist in the clinical setting.

Abbreviations: ATP, adenosine triphosphate; BMOL, bipotential murine oval liver; cIAP, cellular inhibitor of apoptosis protein; DHE, dihydroethidium; DLC, delocalized lipophilic cation; HCC, hepatocellular carcinoma; [(iPr_2-Im)$_2$Au]Cl, *bis*(1,3-di-isopropylimidazol-2-ylidene)gold(I) chloride; (iPr_2-Im)AuCl, 1,3-di-isopropylimidazol-2-ylidenegold(I) chloride; LPC, liver progenitor cell; MnSOD, manganese superoxide disumutase; $\Delta\psi_m$, mitochondrial membrane potential; PIL, p53-immortalized liver; ROS, reactive oxygen species; TPMP, methyltriphenylphosphonium; Yap, yes-associated protein.

Here, we show that an increased expression of the antiapoptotic proteins cellular inhibitor of apoptosis protein (cIAP) and yes associate protein (Yap) in the tumorigenic PIL2 cells may contribute to their resistance to apoptosis. Furthermore, we show that the tumorigenic PIL2 cells have an increased expression of specific mitochondrial proteins and elevated $\Delta\psi_m$ compared with non-tumorigenic PIL4 cells, suggesting that they can be useful models to delineate the role of mitochondrial dysfunction in tumorigenesis. We selected one example from a series of cationic gold(I) *N*-heterocyclic carbene compounds that have been designed as potential new anticancer agents able to target mitochondria and investigated its selectivity for cancer cells based on the difference in $\Delta\psi_m$. We show that the tumorigenic LPCs have an elevated $\Delta\psi_m$ that selectively sensitizes them to this cationic gold(I) compound, which accumulates in mitochondria of cells driven by the $\Delta\psi_m$. Our study demonstrates that the non-tumorigenic and tumorigenic LPCs are useful models for future research in developing and screening for mitochondria-targeted chemotherapeutics that selectively target tumor cells.

Materials and methods

Reagents

Bis(1,3-di-isopropylimidazol-2-ylidene)gold(I) chloride ([$(iPr_2Im)_2$Au]Cl) was synthesized and characterized as reported elsewhere (25) and 10 mM stock solutions were prepared in water. 1,3-Di-isopropylimidazol-2-ylidenegold(I) chloride ((iPr_2Im)AuCl) was synthesized according to the published procedures (26) and 1 mM stock solutions were prepared in 1% dimethyl sulfoxide in water. Cell culture supplements and media, methyltriphenylphosphonium (TPMP) and carbonyl cyanide 4-(trifluoromethoxy)phenylhydrazone were from Sigma, St Louis, MO, USA. The fluorogenic substrates 7-amino-4-methylcoumarin-labeled peptide (DEVD–AMC) and 7-amido-4-trifluoromethylcoumarin-labeled peptide (Ac-LEHD–AFC) were from Calbiochem, Darmstadt, Germany. The JC-1, dihydroethidium (DHE) and amplex red dyes were obtained from Invitrogen (Melbourne, Australia). [^{3}H]TPMP iodide was from American Radiochemicals, St Louis, MO, USA. Mouse 430.20 microarray chips were produced by Affymetrix (Santa Clara, CA). Annexin V–FLUOS, Universal Probe Library, probes master mix and 384-well plates were from Roche, Basel, Switzerland.

Cell culture

Mouse PIL and bipotential murine oval liver (BMOL) (27) cell lines were cultured at 37°C under humidified 95% air/5% CO_2 in Williams' E medium containing 2 mM glutamine, penicillin (100 U/ml), streptomycin (100 μg/ml), humulin (10 μg/ml), epidermal growth factor (20 ng/ml), insulin-like growth factor II (30 ng/ml) and 5% fetal bovine serum.

Apoptosis assays

To measure caspase activities, 10^5 PIL2, PIL4 and BMOL cells were plated overnight in 24-well cell culture plates and then incubated with 4 μM [$(iPr_2Im)_2$Au]Cl for up to 24 h. Caspase-3 and caspase-9 activities were measured as described before (24).

To measure apoptosis by Annexin V–fluorescein isothiocyanate staining, 10^3 cells grown on collagen-coated glass coverslips (in 24-well plates) were incubated in the presence or absence of 50 μM ceramide at 37°C for 4 h. At the end of the incubation, cells were collected by trypsin treatment and centrifugation (1000*g* for 5 min). The cells were resuspended in 1 ml of binding buffer (10 mM 4-(2-hydroxyethyl)-1-piperazineethanesulfonic acid–NaOH, pH 7.4, 150 mM NaCl, 2.5 mM $CaCl_2$, 1 mM $MgCl_2$ and 4% bovine serum albumin) containing 1.25 μl Annexin V–fluorescein isothiocyanate (200 μg/ml) and incubated for 15 min at room temperature in the dark. The cells were collected (1000*g* for 5 min) and gently resuspended in 0.5 ml binding buffer containing 10 μl propidium iodide (30 μg/ml). Cells undergoing apoptosis were quantitated using a Becton Dickinson FACSCanto flow cytometer.

Microarray analysis

RNA was isolated from 10^7 cells with TRIzol Reagent (Invitrogen). Total RNA concentrations were determined with a Biophotometer (Eppendorf, Sydney, Australia). Reverse transcription, RNA labeling (5 μg of total RNA), hybridization to Mouse 430.20 microarray chips (Affymetrix) and scanning were performed according to the manufacturer's instructions (Affymetrix; http://www.affymetrix.com). Hybridization plots and poly A plots were examined to ensure quality control for all the three arrays. Raw fluorescence values were imported into AVADIS 4.3 Prophetic and MAS 5.0 normalization was used to determine present versus absent calls, i.e. expressed or not expressed. MAS 5.0 compares the ratio of raw fluorescence between perfect match and mismatch probe set identifiers. A present call required that probe set identifiers were present in two of three arrays with a P value of ≤ 0.05. The robust mass analysis algorithm was then used to summarize the probe set values and generate fluorescent values for the probe set identifiers. A list of 23 238 present probe sets was generated (supplementary Table 1 is available at *Carcinogenesis* Online). Data were then exported to excel and gene expression in PIL2 was compared against gene expression in PIL4 and BMOL. Probe sets with $\geq$2-fold upregulation and $\geq$2-fold downregulation were determined using fluorescent values (supplementary Table 2 is available at *Carcinogenesis* Online). Gene ontology lists were sourced from Mouse Genome Informatics (http://www.informatics.jax.org/) and cross-referenced with probe set identifiers to calculate the numbers of genes whose transcript abundance changed between the different cell types (Figure 2).

Quantitative reverse transcription–polymerase chain reaction

The transcript abundance of genes encoding cIAP1, Yap and manganese superoxide disumutase (MnSOD) was validated on RNA from the three cell lines. First-strand complementary DNA was prepared from 5 μg of total RNA, using ThermoScript (Invitrogen) and random hexamers. Two microliters of first-strand complementary DNA was used as a template in the subsequent polymerase chain reaction that was performed on the Roche LightCycler 480 with 0.5 μM gene-specific primers: 5′-CCGAGGAGAAGTACCACGAG-3′ and 5′-TATGTCCCCCACCATTGAAC-3′ for MnSOD, 5′-GCTAGATATCCTCATCTTCTTGAGC-3′ and 5′-CCAAAATGCACCACTGTCTCT-3′ for cIAP1, 5′-ACAGCAAATGCTCCAAAATGT-3′ and 5′-CATCCTGCTCCAGTGTAGGC-3′ for Yap and 5′-TCTGTTTTCCCGTGACACAA-3′ and 5′-GCCAGGCGTAGCAACAATAACA-3′ for mannose 6 phosphate receptor; the following Universal probe library were used: #41 for MnSOD, #71 for Yap and #2 for cIAP1 and M6pr protein was used as housekeeping gene with probe #71 and probes master mix in a final volume of 10 μl per reaction, according to the manufacturer's instructions. All polymerase chain reactions were performed in triplicate. Analysis was conducted using LightCycler 480 analysis software.

Mitochondrial isolation

Mitochondria were prepared from 10^7 cells grown overnight in 15 cm^2 dishes and isolated as described before (24).

Immunoblotting

Specific proteins were detected using a mouse MnSOD monoclonal antibody (diluted 1:2000, Transduction Laboratories, Franklin Lakes, NJ, USA), rat cIAP1 monoclonal antibody (diluted 1:1000 in 5% skim milk powder in phosphate-buffered saline) and rabbit Yap polyclonal antibody (diluted 1:1000, Cell Signaling Technology, Danvers, MA, USA). Control immunoblots of the cytosol fractions against the anti-mouse MnSOD antibody showed complete separation of the mitochondria from the cytosol. Control immunoblots against β-actin (diluted 1:1000, Sigma, A-1978) were used to confirm normalized protein loading.

Superoxide and hydrogen peroxide measurements

For DHE measurements, 10^3 cells per well were plated in black 96-well tissue culture plates. After 3 days, the growth medium was replaced with fetal bovine serum-free medium containing 10 μM DHE and incubated for 45 min at 37°C. For amplex red measurements, 10^3 cells were plated in 96 wells and allowed to attach overnight. The growth medium was replaced with 100 μl phosphate-buffered saline containing 100 μM amplex red and 0.2 U/ml horseradish peroxidase and incubated for 30 min at 37°C; the incubation medium was then removed and 100 μl of phosphate-buffered saline/0.1% Triton X-100 was added to each well. For positive control incubations, the cells were treated with 4 μg/ml rotenone. The fluorescent signal was measured in a BMG Labtech Fluostar Optima plate reader ($\lambda_{Excitation}$ = 544 nm and $\lambda_{Emission}$ = 590 nm). The protein concentration was determined using the bicinchoninic acid assay and the fluorescence was normalized for protein amount for the DHE measurements. The hydrogen peroxide concentration was determined using a standard curve.

Measurement of $\Delta\psi_m$

For membrane potential measurements, 10^5 cells per well were plated in black 96-well tissue culture plates. The following day, the growth medium was replaced with fresh medium containing 4 μM [$(iPr_2Im)_2$Au]Cl and incubated up to 48 h. The $\Delta\psi_m$ was measured as described before (24). The $\Delta\psi_m$ of 10^6 cells grown in 10 cm dishes and treated with the 2 μM of JC-1 was quantified using a Becton Dickinson FACSCanto flow cytometer with a 488 nm excitation laser. The green emission was detected with a 530/30 band pass filter and red emission was detected with a 585/42 band pass filter.

The $\Delta\psi_m$ was quantitated by incubating mitochondria in 120 mM KCl, 10 mM 4-(2-hydroxyethyl)-1-piperazineethanesulfonic acid, 1 mM ethylene glycol tetraacetic acid, pH 7.2, supplemented with 10 mM succinate and 4 μg/ml rotenone and 0.5 μM TPMP supplemented with [^{3}H]TPMP (100 nCi/ml) at 37°C for 5 min. At the end of the incubation, the mitochondria were pelleted by

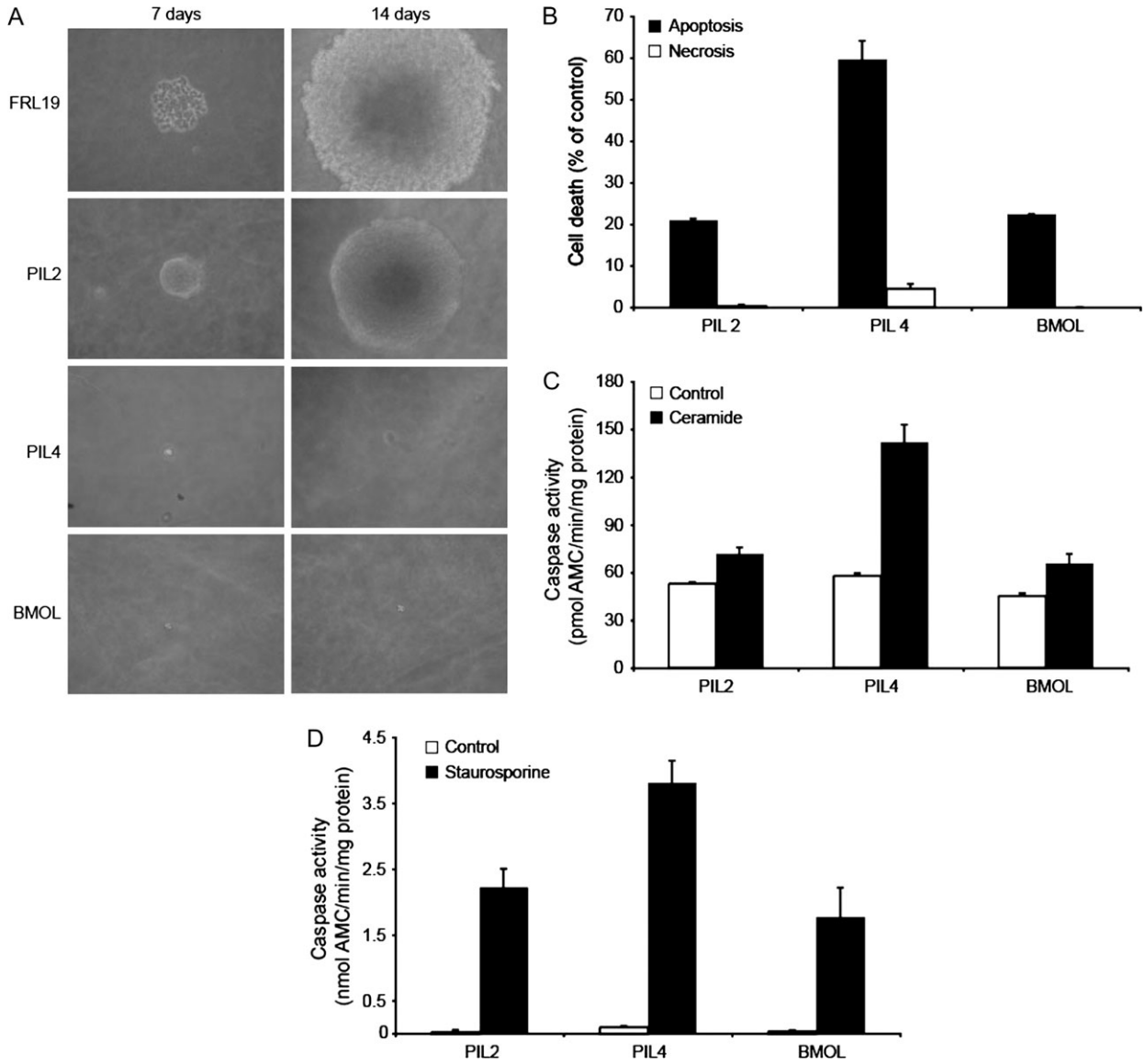

Fig. 1. PIL2 cells are tumorigenic and resistant to apoptotic stimuli. (**A**) Cell lines were grown in semisolid agar and colony formation was measured following 7 and 14 days. (**B**) Cells incubated with 50 μM ceramide were harvested and the proportion of annexin V- and propiduim iodide-positive cells was analyzed by flow cytometry. Data are expressed as percent of control incubations in the absence of ceramide. Cells were treated with either 50 μM ceramide (**C**) or 2.5 μM staurosporine (**D**) for 3 h. After the incubation, cell lysates were harvested and assayed for caspase-3 activity, measured as the rate of DEVD-AMC cleavage. Control incubations were carried out in the absence of apoptosis inducers. Data are means ± SDs of at least four separate experiments.

centrifugation (10 000*g* for 20 s), and the amounts of TPMP in the pellet and supernatant were quantitated by scintillation counting (28). The $\Delta\psi_m$-independent TPMP accumulation was determined by parallel incubations supplemented with carbonyl cyanide 4-(trifluoromethoxy)phenylhydrazone (1 μM) and was subtracted from the accumulation by coupled mitochondria to give the $\Delta\psi_m$-dependent TPMP accumulation. The $\Delta\psi_m$ was calculated as an accumulation ratio in the units of [(TPMP per milligram of protein)/(TPMP per microliter of supernatant)] assuming a mitochondrial volume of 0.5 μl/mg protein, and that 60% of intramitochondrial TPMP was membrane bound (29,30).

Measurement of mitochondrial uptake

Confluent cells grown in 15 cm^2 dishes were incubated with $[(iPr_2Im)_2Au]Cl$ (4 μM) at 37°C for 3 h and at the end of the incubation mitochondria were isolated. Mitochondrial pellets were resuspended in 350 μl water and 300 μl was digested in 70% HNO_3 (500 μl) at 70°C for 2 h. The samples were then diluted 1:10 in water for inductively coupled plasma mass spectrometry (ICP–MS). Gold analysis was carried out using an Agilent 7500cs ICP–MS with a micromist concentric nebulizer, and a double-pass spray chamber maintained at 2°C. Gold was read at up to 1 ng/ml and the sensitivity limit of detection was 10 pg/ml (95% confidence limit). Protein concentrations of cell fractions were determined by the bicinchoninic acid assay using bovine serum albumin as a standard.

Cell viability assays

For cell growth studies, 70% confluent cells in 96-well plates were incubated for 72 h with 200 μl of growth medium without phenol red containing increasing concentrations of gold compound. Cell death was determined using the cell titer assay following the manufacturer's instructions (Promega, Sydney, Australia G3580). Cell death was determined using the ATPlite luminescence assay kit (PerkinElmer, Waltham, MA, USA) according to the manufacturer's instructions. To measure the cell growth, 10^4 cells were grown in 24-well plates overnight. The following day when the cells were 40% confluent, 4 μM $[(iPr_2Im)_2Au]Cl$ was added and cell growth was measured every 12 h for up to 72 h using a Innovatis Cellscreen automated cell counter (31). Data are means ± SDs of three independent experiments.

Results

Only tumorigenic LPCs grow in semisolid medium

LPC lines were established and some were shown to be tumorigenic, whereas others failed to produce tumors in immunodefficient nude mice (32). We confirmed that sublines derived from these original cell

A

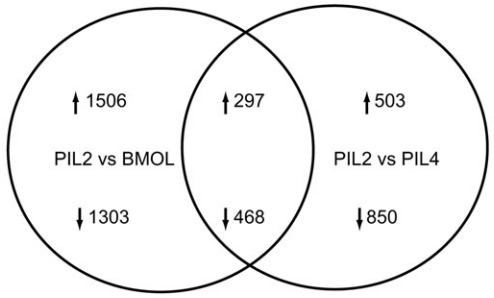

C

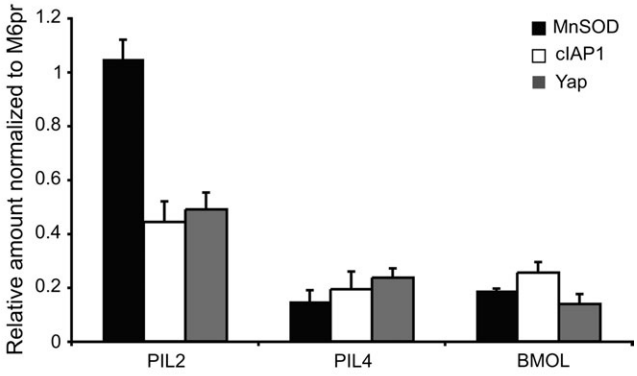

B

Upregulated genes		PIL2 Versus PIL4	PIL2 Versus BMOL	PIL4 Versus BMOL
cIAP2	Baculoviral IAP repeat-containing 2	2.8	3.4	1.2
Sod2	Superoxide dismutase 2, mitochondrial	2.2	2.8	1.3
Hspa1b	Heat shock protein 1B	3.0	3.8	1.3
Casp12	Caspase 12 / hypothetical protein LOC100044205	6.7	5.3	0.8
Jak2	Janus kinase 2	2.2	2.5	1.2
Egln3	EGL nine homolog 3 (C. elegans)	2.2	11.2	5.2
Downregulated genes				
Sgk3	Serum/glucocorticoid regulated kinase 3	5.4	2.6	0.5
Btg2	B-cell translocation gene 2, anti-proliferative	3.0	5.5	1.8
Aldh1a1	Aldehyde dehydrogenase family 1, subfamily A1	3.8	4.1	1.1
Cadm1	Cell adhesion molecule 1	2.4	4.9	2.0
Proc	Protein C	3.9	3.3	0.9
Peg3	Paternally expressed 3	17.4	11.4	0.7
Il18	Interleukin 18	2.8	2.3	0.8
Traf3	Tnf receptor-associated factor 3	12.9	8.8	0.7
Perp	PERP, TP53 apoptosis effector	8.0	7.8	1.0
Housekeeping genes				
β-Actin	β-Actin	1.0	1.2	1.3
M6pr	Maltose 6 phosphate receptor	1.0	1.0	1.0

Fig. 2. Differences in gene expression between tumorigenic and non-tumorigenic LPC. (**A**) Venn diagram showing the total number of genes after multiple probes representing one gene was removed in PIL2 cells that had changes in their expression compared with PIL4 and BMOL cells. (**B**) Microarray analysis of PIL2, PIL4 and BMOL cells. The difference in the expression of genes involved in apoptosis in PIL2 cells compared with PIL4 and BMOL cells is shown. (**C**) Quantitative reverse transcription–polymerase chain reaction of cIAP1, Yap and MnSOD expression in PIL2, PIL4 and BMOL cells. Data are means of three separate experiments.

lines retained their phenotypes by growing them in a semisolid agar. The tumorigenic phenotype of the PIL2 cell line was similar to the FRL19 cell line (33) after 7 and 14 days of growth in the soft agar (Figure 1A). In contrast, there was no growth of the PIL4 cell line comparable with that of the p53 wild-type non-tumorigenic cell line (BMOL) (Figure 1A). Taken together, these data indicate that the PIL2 cell line is tumorigenic and the PIL4 cell line is non-tumorigenic, despite their lack of the tumor suppressor protein p53 (32).

Tumorigenic PIL2 cells evade apoptosis

One of the hallmarks of tumorigenic cells is their ability to resist programmed cell death (34). To determine whether there was a difference in resistance of the PIL cell lines to apoptotic stimuli, cell death was measured either by annexin and propidium iodide staining or caspase-3 activation. At least 60% of PIL4 cells undergo programmed cell death following ceramide treatment compared with 20% of PIL2 cells (Figure 1B). Less than 5% of cells died by necrosis in both cell lines. Caspase-3 measurements further indicate that the PIL4 cells apoptose in response to ceramide but not the PIL2 cells (Figure 1C). Furthermore, we show that caspase-3 activity is significantly higher in the PIL4 cells in response to the protein kinase C inhibitor, staurosporine, compared with that of the PIL2 cells (Figure 1D). Collectively, these findings suggest that the PIL2 cell line possesses a common feature of tumorigenic cells, which is the ability to resist programmed cell death.

Significant differences in gene expression pattern exist between tumorigenic and non-tumorigenic LPC

A two-step approach was carried out to identify genes that differed in expression between tumorigenic and non-tumorigenic cell lines.

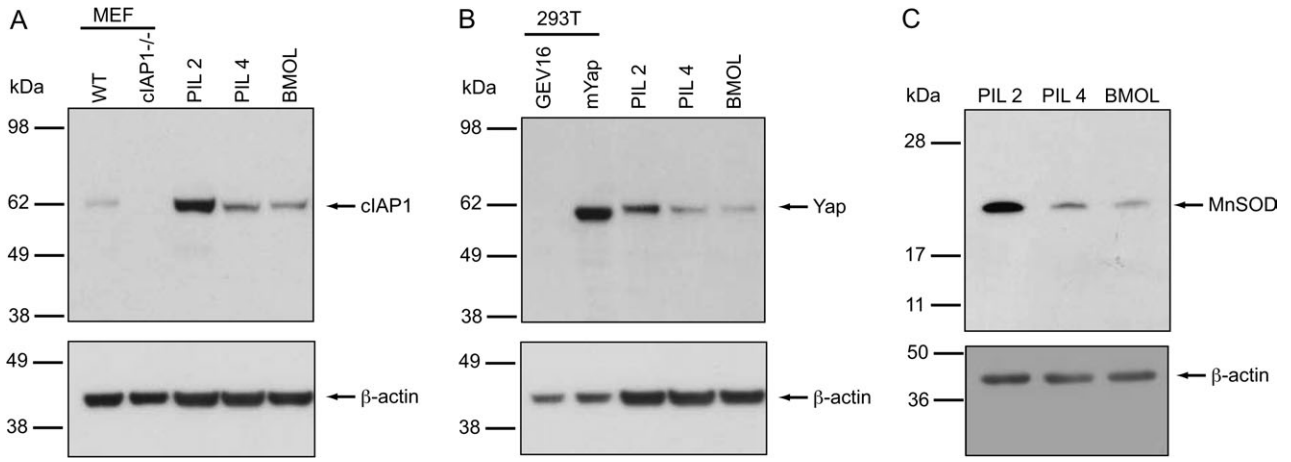

Fig. 3. cIAP1, Yap and MnSOD have increased expression in PIL2 cells compared with PIL4 and BMOL. Cell lysates (20 μg protein per lane) were resolved by sodium dodecyl sulfate–polyacrylamide gel electrophoresis and analyzed for cIAP1 (**A**), Yap (**B**) and MnSOD (**C**) protein expression by immunobloting. Wild-type and cIAP1−/− mouse embryonic fibroblasts lysates were included as controls for the cIAP1 antibody. Lysates of 293T cells transiently transfected with mouse yes associated protein or inducible transcriptional activator Gal4ER^{T2}VP16 complementary DNAs were included as controls for the Yap antibody. The figure shows a typical experiment repeated on at least three separate cell preparations.

Firstly, differences in transcript abundance for a variety of genes were determined using microarray analysis (supplementary Table 1 is available at *Carcinogenesis* Online). In the PIL2 cells, 765 genes were identified that had significantly altered expression pattern to that of PIL4 and BMOL cells (Figure 2A). Secondly, to investigate the mechanisms underlying the differential sensitivity to apoptotic stimuli between the tumorigenic and non-tumorigenic cells, we used the mouse genome informatics ontology classification to identify a subset of 15 differentially expressed genes that are involved in apoptosis (Figure 2B). The antiapoptotic protein cIAP1 for which overexpression has been linked to liver tumorigenesis (35) was increased in PIL2 cells by 2.8-fold compared with PIL4 and 3.4-fold compared with BMOL. Because Yap has been shown to be overexpressed with cIAP1 and synergistically contribute to liver tumorigenesis (35), we examined Yap expression and observed that its transcript level was elevated in PIL2 cells by 2.3-fold compared with BMOL and by 1.6-fold compared with PIL4 (supplementary Table 1 is available at *Carcinogenesis* Online). Interestingly, the transcript for the mitochondrial antioxidant enzyme MnSOD was elevated in the PIL2 cells by 2.2-fold compared with PIL4 and by 2.8-fold compared with BMOL. The amount of the housekeeping transcripts for the mannose 6 phosphate receptor and β-actin in the three cell lines was similar (Figure 2B). The expression level of genes encoding cIAP1, Yap and MnSOD was confirmed by quantitative reverse transcription–polymerase chain reaction (Figure 2C).

We used immunoblotting to confirm that the difference in cIAP1, Yap and MnSOD expression between the three cell lines observed with the microarray occurred at the protein level. The expression of the mitochondrial antiapoptotic protein cIAP1 was significantly increased in the PIL2 cells compared with PIL4 and BMOL (Figure 3A). The expression of the Yap antiapoptotic protein was similarly elevated in the PIL2 cells compared with PIL4 and BMOL (Figure 3B). MnSOD has been shown to be elevated in many cancer cells including hepatoma cells (36) and consistent with this observation, it was elevated in the PIL2 cells compared with the PIL4 and BMOL cells (Figure 3C). The amount of the housekeeping protein β-actin in the three cell lines was similar (Figure 3).

Increased MnSOD levels are a result of elevated reactive oxygen species in the PIL2 cells

Expression of the mitochondrial antioxidant enzyme MnSOD is typically increased in response to an elevated production of superoxide within mitochondria. We show that the superoxide levels are >1.5-fold higher in the PIL2 cells compared with the PIL4 and BMOL cells (Figure 4A). This is consistent with our finding that hydrogen peroxide production in the PIL2 cells is 2-fold higher than in the PIL4 and BMOL cells (Figure 4B).

Tumorigenic PIL cells have increased $\Delta\psi_m$

Mitochondrial superoxide is produced when electrons escape the respiratory complexes and react with molecular oxygen, which can occur when the $\Delta\psi_m$ is high. We observed a consistently greater accumulation of the JC-1 dye in the PIL2 cells, suggesting that their $\Delta\psi_m$ was elevated compared with PIL4 and BMOL cells (Figure 4C). Furthermore, we used the radiolabeled lipophilic phosphonium cation TPMP to accurately quantify the $\Delta\psi_m$ of the three cell lines. The $\Delta\psi_m$ of PIL2 cells is at least 40 mV higher than the $\Delta\psi_m$ of PIL4 and BMOL cells (Figure 4D). These results indicate that the tumorigenic LPCs have an increased $\Delta\psi_m$ compared with the two non-tumorigenic lines.

A new gold lipophilic cation selectively targets mitochondria of tumorigenic PIL cells

DLCs have been used as a new approach to cancer chemotherapy that exploits their selective accumulation in mitochondria of cancer cells as a consequence of the $\Delta\psi_m$ that is a shared feature for many tumor cell lines (11,13). For a series of cationic gold(I) *N*-heterocyclic carbene complexes of the form $[R_2Im)_2Au]^+$, the lipophilicity varies with the nature of the alkyl substituents (R) (25). We selected the compound $[(iPr_2Im)_2Au]Cl$, which has intermediate lipophilicity, and compared the toxicity with that of the related neutral chloro compound $(iPr_2Im)AuCl$ (Figure 5A). We compared the toxicity effects of these compounds on all the three cell lines (Figure 5B and C). $[(iPr_2Im)_2Au]Cl$ selectively inhibited PIL2 cell growth at concentrations <6 μM (Figure 5B), whereas $(iPr_2Im)AuCl$ inhibited the growth of all the three cell lines at similar concentrations (Figure 5C). These data show that $[(iPr_2Im)_2Au]Cl$ selectively inhibits the growth of PIL2 cells but not the non-tumorigenic PIL4 and BMOL cells.

To show that the lipophilic, cationic gold compound accumulates in mitochondria of cells driven by the $\Delta\psi_m$, PIL2 cells were treated with increasing concentrations of $[(iPr_2Im)_2Au]Cl$ and the amount of gold present in their mitochondria was measured by ICP–MS. Gold within mitochondria increased with increasing concentrations of $[(iPr_2Im)_2Au]Cl$ (data not shown). At a concentration of 4 μM, which inhibits cell growth by >50%, >80% of the measured gold is found within the mitochondria of cells (Figure 5D). Dissipating the $\Delta\psi_m$ with the uncoupler carbonyl cyanide 4-(trifluoromethoxy)phenylhydrazone shifts the distribution of the gold to the cytoplasm with only ∼18% remaining in mitochondria (Figure 5D). Taken together, these data indicate that $[(iPr_2Im)_2Au]Cl$ accumulates in mitochondria

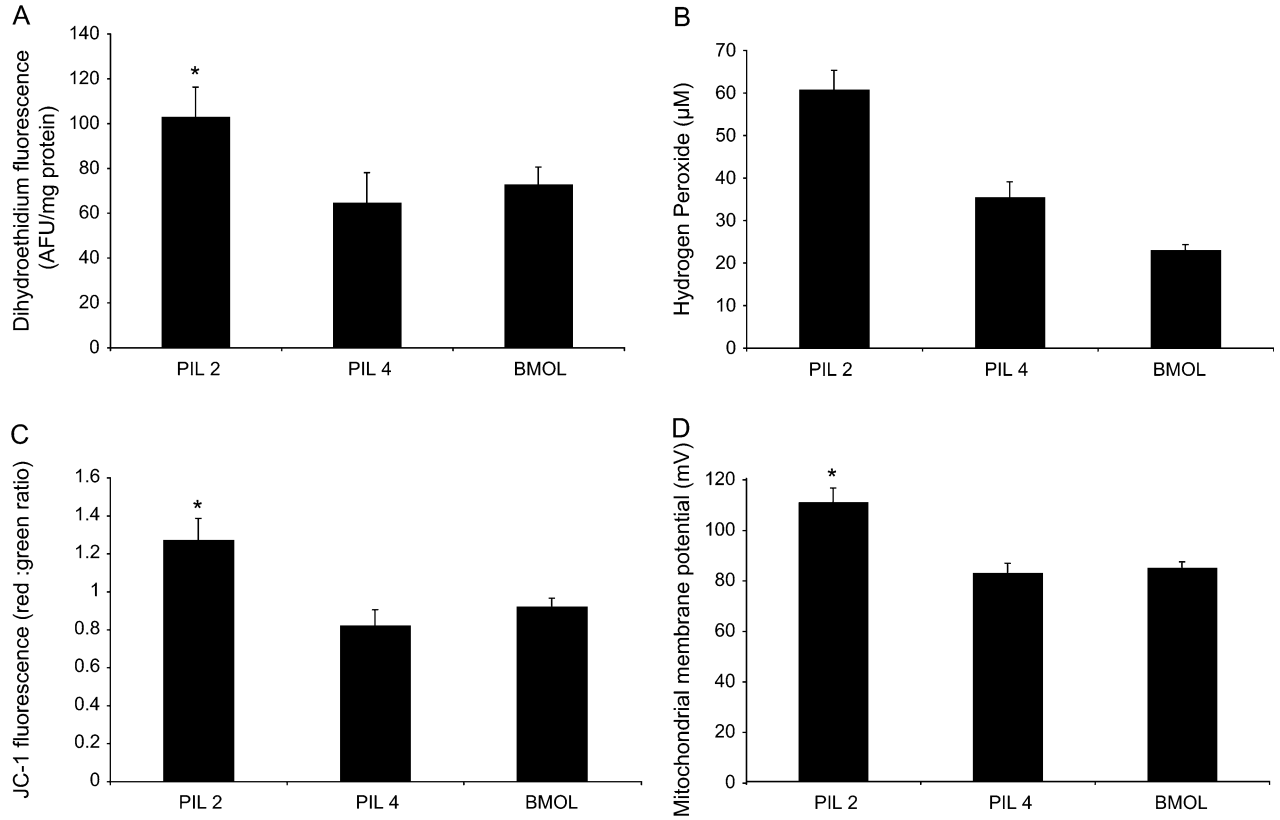

Fig. 4. Tumorigenic PIL2 cells have an increased production of ROS and an elevated $\Delta\psi_m$. (**A**) Superoxide was measured by incubating cells with 10 μM DHE for 45 min at 37°C. At the end of the incubation, the cells were lysed and the fluorescence was measured. (**B**) Hydrogen peroxide was assayed by incubating the cells with 100 μM amplex red and 0.2 U/ml horseradish peroxidase for 30 min at 37°C and measuring the released fluorescence at the end of the incubation. Concentration was determined using hydrogen peroxide as a standard. (**C**) The $\Delta\psi_m$ in cells was measured using the fluorescent dye JC-1 and expressed as a ratio of red to green fluorescence. (**D**) Mitochondria were isolated from the three cell lines by homogenization and differential centrifugation, and their membrane potential was measured from the distribution of [^{3}H]TPMP while respiring on succinate. $^*P$ 0.05 compared with PIL4 and BMOL cells by a two-tailed paired Student's *t*-test. Data are means ± SDs of at least four separate experiments.

of cells driven by the $\Delta\psi_m$ and its uptake is selective for the mitochondria of tumorigenic cells presumably as a result of the increased $\Delta\psi_m$.

Selective inhibition of tumorigenic PIL cell growth by [(iPr$_2$Im)$_2$Au]Cl

To further show that [(iPr$_2$Im)$_2$Au]Cl selectively inhibits the PIL2 cell growth, we treated all the three cell lines with the compound over 72 h and assessed cell growth by the cell screen assay. The growth of PIL2 cells was inhibited by 50% after a 48 h incubation with the gold compound, but not the growth of the PIL4 and BMOL cells (Figure 6A). The loss of >80% of total ATP after 72 h in the PIL2 cells but not in PIL4 and BMOL cells further confirmed the selective toxicity of the gold compound toward the tumorigenic cells (Figure 6B).

DLCs have been shown to dissipate the $\Delta\psi_m$ upon uptake into mitochondria. Therefore, we measured the $\Delta\psi_m$ of the three cell lines in the absence and presence of [(iPr$_2$Im)$_2$Au]Cl using the JC-1 dye. The $\Delta\psi_m$ of the PIL2 cells dissipated over time in the presence of 4 μM [(iPr$_2$Im)$_2$Au]Cl, consistent with the uptake of the compound into mitochondria of the cells (Figure 6C). This decrease suggests that this gold compound has a sustained and selective uncoupling effect on the $\Delta\psi_m$ of the PIL2 cells after a 12 h incubation, whereas the $\Delta\psi_m$ of PIL4 and BMOL cells was unaffected.

[(iPr$_2$Im)$_2$Au]Cl selectively induces apoptosis in the tumorigenic PIL cells via mitochondria

We measured the amount of caspase-3 activation, as a marker of apoptosis, to clarify whether [(iPr$_2$Im)$_2$Au]Cl leads to selective cell death in the PIL2 cells by activating the apoptotic pathway. [(iPr$_2$Im)$_2$Au]Cl causes a marked increase in caspase-3 activation after 12 h of incubation with the PIL2 cells (Figure 6D). In the PIL4 and BMOL cells, there is no caspase-3 activation over the same period, indicating that the effect of [(iPr$_2$Im)$_2$Au]Cl is specific for the PIL2 cell line (Figure 6D). To confirm that [(iPr$_2$Im)$_2$Au]Cl induced apoptosis in the PIL2 cells via mitochondria, we incubated these cells with the gold compound and showed a 3-fold increase in caspase-9 activity (Figure 6D). These data suggest that [(iPr$_2$Im)$_2$Au]Cl causes selective cell death through a mitochondrial apoptotic pathway in the PIL2 cells, but not in the PIL4 or BMOL cells.

Discussion

Delineating differences between tumorigenic and non-tumorigenic cells have been a challenge due to the lack of cell models that allow for comparisons between cells of similar origin, which differ only in their tumorigenicity. We established previously two LPC lines from a p53-null mouse that share the same lineage (32) and in this study, we documented their differences. We show that the PIL2 cells are tumorigenic and grow in soft agar similar to the well-characterized liver-derived tumorigenic cells (37), whereas the PIL4 cells are non-tumorigenic and therefore do not form colonies in soft agar. These findings corroborate a previous study in which the PIL2 cells induced tumors in nude mice, whereas the PIL4 did not (32). The tumorigenic PIL2 cells possess a common feature with the other tumorigenic cells in that they can evade apoptosis. It is interesting to note that BMOL cells do not conform to the expected pattern as they are non-tumorigenic yet insensitive to some apoptotic stimuli. A likely explanation is that they

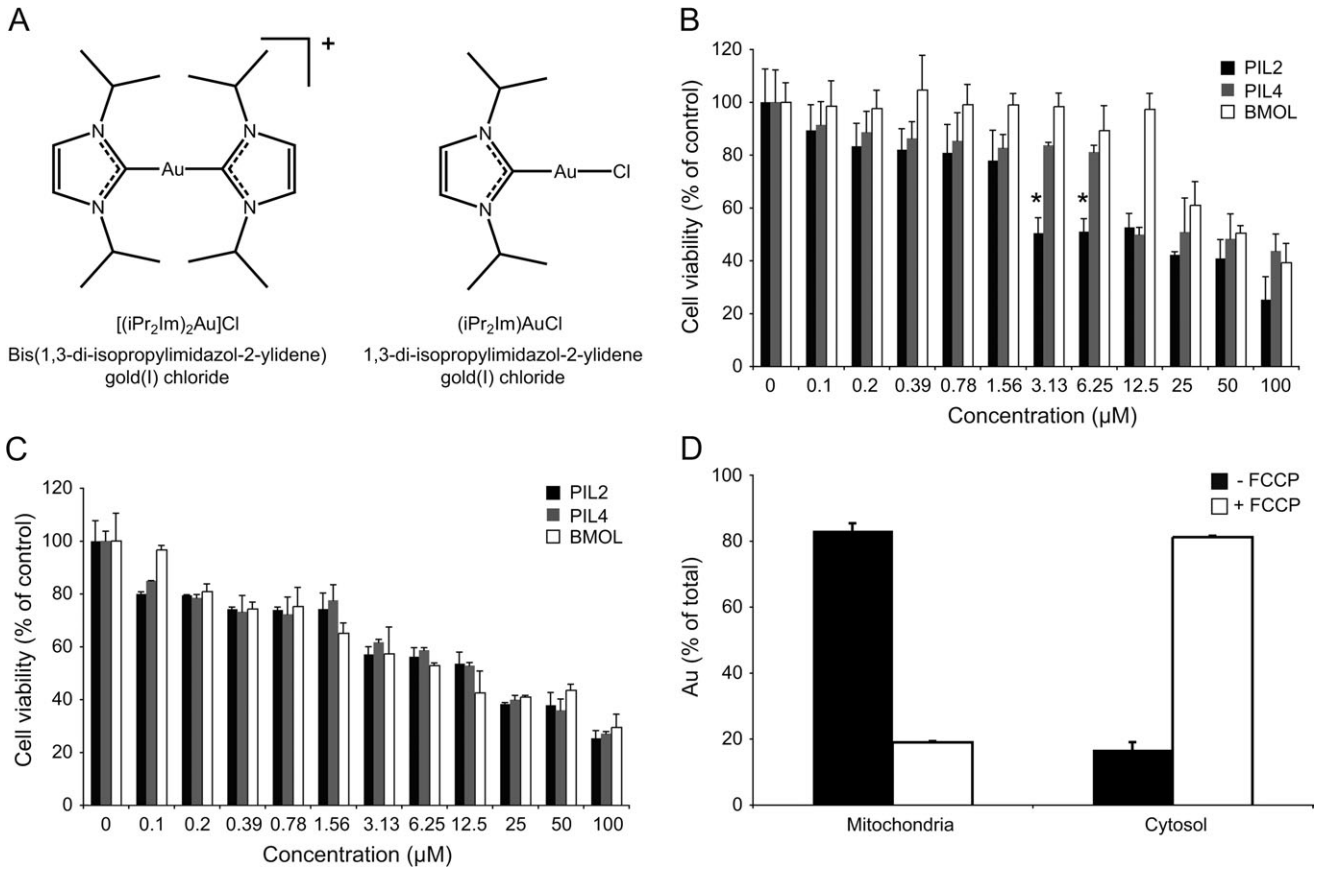

Fig. 5. A new lipophilic, cationic gold(I) *N*-heterocyclic carbene complex selectively accumulates in mitochondria of PIL2 cells driven by the $\Delta\psi_m$. (**A**) Chemical structure of the cationic complex $[(iPr_2Im)_2Au]Cl$ and its neutral analog $(iPr_2Im)AuCl$. The three cell lines were treated with increasing concentrations of either $[(iPr_2Im)_2Au]Cl$ (**B**) or $(iPr_2Im)AuCl$ (**C**) and cell growth was measured after 72 h using a cell titer assay. Data are means ± SDs of four separate experiments. $^*P$ 0.05 compared with PIL4 and BMOL cells by a two-tailed paired Student's *t*-test. (D) $[(iPr_2Im)_2Au]Cl$ uptake into mitochondria within cells. Cells, cytoplasmic and mitochondrial fractions, isolated from the cells treated with $[(iPr_2Im)_2Au]Cl$ were incubated with 70% nitric acid at 70°C for 2 h, diluted 10-fold in water and analyzed for gold content by inductively coupled plasma mass spectrometry (ICP–MS). Gold distribution in mitochondria and cytoplasm of PIL2 cells was measured after treatement with 4 μM $[(iPr_2Im)_2Au]Cl$ for 2 h at 37°C. Control experiments were carried out in the absence of $\Delta\psi_m$ [+carbonyl cyanide 4-(trifluoromethoxy)phenylhydrazone (FCCP)]. Data are means ± SDs of three separate experiments.

possess wild-type p53 and are thus able to invoke normal p53-induced repair pathways upon exposure to apoptosis inducers. This underlines our contention that it is necessary to compare cell lines that differ only in their tumorigenicity in order to delineate cancer genes, which are causal.

To understand the mechanism underlying the enhanced resistance to apoptosis of PIL2 cells, we focused on cIAP1 and Yap that have been shown to cooperate to promote tumorigenesis of LPCs leading to HCC (38). IAP expression has been associated with different cancer phenotypes and their overexpression can inhibit apoptosis induced by different agents (38). In addition, the *Drosophila* homolog of Yap has been shown to promote tumorigenesis by activating the inhibitor of apoptosis gene drosophila inhibitor of apoptosis protein (39), although the exact role of the mammalian Yap in apoptosis is not defined and requires further investigation (40). The increased expression of cIAP1 and Yap messenger RNA and protein in the PIL2 cells compared with PIL4 and BMOL cells corroborates the findings that synergistic overexpression of cIAP1 and Yap can promote liver tumorigenesis (35) and may explain their resistance to apoptotic stimuli.

The mitochondrial electron transport chain is the major site of reactive oxygen species (ROS) production because 2–4% of electrons escape the respiratory complexes and react with molecular oxygen to form superoxide that can form more damaging ROS. The mitochondrial enzyme MnSOD catalyzes the conversion of superoxide anion oxygen to hydrogen peroxide and consequently MnSOD levels are induced in response to an increase in mitochondrial ROS. This was consistent in the PIL2 cells where higher levels of MnSOD correlated with increases in superoxide and hydrogen peroxide. Increased oxidative stress and overexpression of MnSOD have been observed in many different cancer cells including HCC (36,41), suggesting that they may contribute to the tumorigenic phenotype of the PIL2 cells.

High $\Delta\psi_m$ generally results in an increased production of ROS; therefore, we measured the $\Delta\psi_m$ of the three cell lines and showed a 40 mV increase in the $\Delta\psi_m$ of PIL2 cells compared with PIL4 and BMOL cells. Although elevated $\Delta\psi_m$ has been reported for many different cancer cell lines, the mechanism that causes it is unclear (13,42). Differences in $\Delta\psi_m$ could arise as a result of metabolic changes that occur during tumorigenesis including reduced oxidative phosphorylation and inhibition of the ATP synthase activity that reduce dissipation of the proton motive force (22,43). Differences in the expression of mitochondrial genes that have been linked to oncogene expression may contribute to mitochondrial dysfunction and elevated $\Delta\psi_m$ (34,44). Although mitochondrial differences that have been identified to date may explain the basis for the increased $\Delta\psi_m$, they have all been identified in cell lines of different origin and none of the differences are common to all cancer cells. Therefore, the availability of the PIL2 and PIL4 cell lines will provide a useful model for molecular profiling of tumorigenic versus non-tumorigenic cells of similar origin to elucidate the molecular basis of this phenomenon. Identifying the proteins that cause mitochondrial dysfunction in tumorigenic cells will facilitate the development of mitochondria-targeted chemotherapeutics.

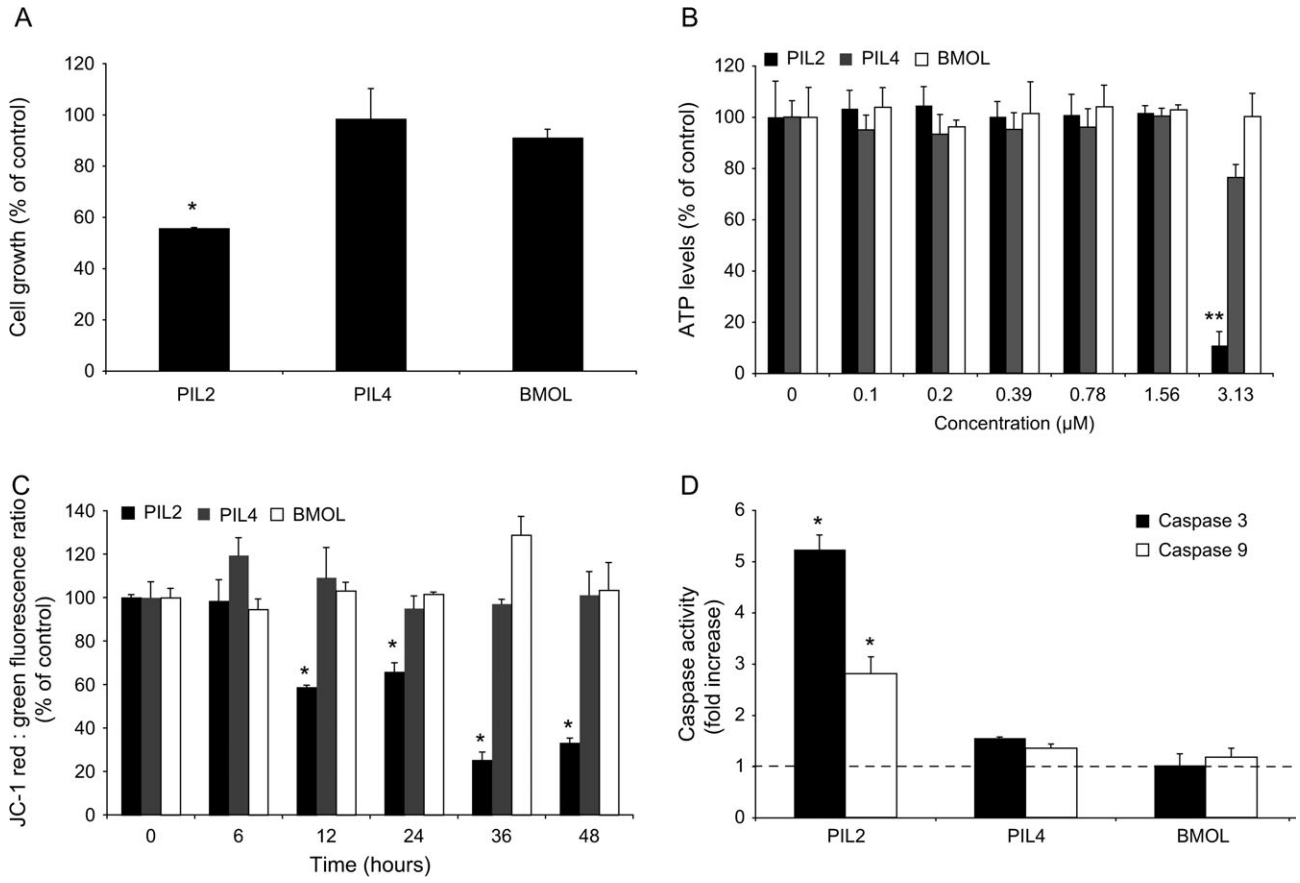

Fig. 6. The lipophilic, cationic gold(I) complex $[(iPr_2Im)_2Au]Cl$ selectively induces apoptosis of PIL2 cells. (**A**) The three cell lines were grown to 40% confluence and then treated with 4 μM $[(iPr_2Im)_2Au]Cl$ and the cell growth was measured using the cell screen assay for up to 72 h. (**B**) Cellular ATP levels of cells treated with 4 μM $[(iPr_2Im)_2Au]Cl$ were measured using the ATPlite luminescence assay kit. (**C**) The effect of 4 μM $[(iPr_2Im)_2Au]Cl$ on $\Delta\psi_m$ in cells was measured using the fluorescent dye JC-1 and expressed as a ratio of red to green fluorescence. Data are expressed as a percent of control of measurements in the absence of $[(iPr_2Im)_2Au]Cl$. Data are means ± SDs of four separate experiments. (**D**) Cells treated with 4 μM $[(iPr_2Im)_2Au]Cl$ were incubated for 12 h. Cell lysates were harvested and assayed for caspase-3 and caspase-9 activity, measured as the rate of DEVD and LEHD cleavage, respectively. Data are expressed as relative fold of activity compared with control measurements in the absence of the compound and are means ± SDs of four separate experiments. $^{*}P$ 0.05 and $^{**}P$ 0.01 compared with PIL4 and BMOL cells by a two-tailed paired Student's *t*-test.

The increased $\Delta\psi_m$ of tumorigenic cells has been used to selectively accumulate drugs into mitochondria of tumor cells with potential anticancer effects (20,22). A variety of DLCs have been shown to have anticancer activities by selectively concentrating in mitochondria, including the F16 compound that selectively induced growth arrest and effectively disrupted the mitochondria of neu oncogene-transformed, immortalized mammary epithelial cells (45–47). In this study, we use a new gold(I) *N*-heterocyclic carbene compound that accumulates selectively in mitochondria driven by the $\Delta\psi_m$ to ascertain its selectivity based on the $\Delta\psi_m$ difference between PIL2 cells compared with PIL4 and BMOL. The octanol/water partition coefficient of $[(iPr_2Im)_2Au]Cl$ ($\log P = -0.83$) (25) lies within the optimal range derived from predictive models for the selective accumulation of DLCs in cancer cells based on lipophilicity (48,49) and as a result of this and its positive charge, this complex selectively accumulated in mitochondria of PIL2 cells. This compound selectively depolarized the $\Delta\psi_m$ of PIL2 cells most probably as a result of its increased accumulation due to the elevated $\Delta\psi_m$. $[(iPr_2Im)_2Au]Cl$ was selectively toxic to the PIL2 cells but not PIL4 and BMOL cells. The compound inhibited PIL2 cell growth by at least 50% and reduced the cellular ATP supply by 90%, which may exacerbate cell death. The activation of the caspase-9 and caspase-3 in the PIL2 cells treated with the gold compound confirmed that programmed cell death was mediated via mitochondria. This selective anticancer activity of $[(iPr_2Im)_2Au]Cl$ is consistent in other breast cancer cell lines compared with normal breast cells (J.L.Hickey, R.A.Ruhayel, P.J.Barnard, M.V.Baker, S.J.Berners-Price and A.Filipovska, in preparation). The neutral compound $(iPr_2Im)AuCl$ induced non-selective cell death in all the three cell lines, suggesting a mechanism of action different from $[(iPr_2Im)_2Au]^+$ that does not depend on the $\Delta\psi_m$. The chloride ligand is probably to be readily substituted with protein thiols and selenols, similar to related gold(I) phosphine complexes such as auranofin (21), resulting in cell death by altering the cellular redox state. This further suggests that the selectivity of $[(iPr_2Im)_2Au]Cl$ for the tumorigenic cells is due to its lipophilic, cationic nature that facilitates its accumulation into cancer cells with increased $\Delta\psi_m$. Although DLCs such as MKT-077 have proven highly toxic in clinical trials, the high selectivity for cancer cells of some DLCs, including gold(I) compounds with phosphine and *N*-heterocyclic ligands, suggests that targeting mitochondria of cancer cells may have significant anticancer therapeutic potential and should be further developed. In addition, the PIL2 and PIL4 cell lines are useful models for screening chemotherapeutics that use the increase in $\Delta\psi_m$ to target mitochondria of tumor cells.

Recent developments ascribing a central role for mitochondria as regulators of cell death have stimulated enormous interest in targeting mitochondria in new approaches to cancer chemotherapy (34). Inactivation of the tumor suppressor gene p53 and overexpression of anti-apoptotic proteins, such as Bcl-2, are common features of tumor cells that confer resistance to apoptotic stimuli. Therefore, the selective

induction of the apoptotic pathway that is evaded in cancer cells has great potential for the development of new generation of mitochondria-targeted chemotherapeutics. In addition, the selective effect of $[(iPr_2Im)_2Au]Cl$ on the tumorigenic cells suggests a causal link between expression of particular oncogenes, such as cIAP1 and Yap, increased $\Delta\psi_m$ and the response to DLC may exist. Enhanced production of ROS has also been linked to neoplasmic transformation; however, a mechanistic link between increased expression of antiapoptotic genes and increased $\Delta\psi_m$ and mitochondrial ROS has not been made to date. We have established that PIL2 and PIL4 LPCs are suitable models for such future studies that aim to elucidate the role of mitochondrial dysfunction in the onset of tumorigenesis.

Supplementary material

Supplementary Tables 1 and 2 can be found at http://carcin.oxfordjournals.org/

Funding

National Health and Medical Research Council; Cancer Council of Western Australia; Australian Research Council.

Acknowledgements

We thank Mr James Hickey for the synthesis of the Au(I) carbene complex, Dr John Silke and Diep Chau from La Trobe University for the cIAP1 antibody, Dr Kathryn Heel for assistance with the FACS, Dr Kate Howell for assistance with the microarray analysis and the ICP–MS group in The Centre for Forensic Science at the University of Western Australia for their help with the ICP–MS analysis. We thank Ms Janina Tirnitz-Parker for establishing and providing the BMOL cells.

Conflict of Interest Statement: None declared.

References

1. Hsia,C.C. *et al*. (1992) Occurrence of oval-type cells in hepatitis B virus-associated human hepatocarcinogenesis. *Hepatology*, **16**, 1327–1333.
2. Lowes,K.N. *et al*. (1999) Oval cell numbers in human chronic liver diseases are directly related to disease severity. *Am. J. Pathol.*, **154**, 537–541.
3. Fausto,N. (1990) Oval cells and liver carcinogenesis: an analysis of cell lineages in hepatic tumors using oncogene transfection techniques. *Prog. Clin. Biol. Res.*, **331**, 325–334.
4. Knight,B. *et al*. (2000) Impaired preneoplastic changes and liver tumor formation in tumor necrosis factor receptor type 1 knockout mice [in process citation]. *J. Exp. Med.*, **192**, 1809–1818.
5. Petrosillo,G. *et al*. (2007) Mitochondrial dysfunction in rat with nonalcoholic fatty liver involvement of complex I, reactive oxygen species and cardiolipin. *Biochim. Biophys. Acta*, **1767**, 1260–1267.
6. Sun,A.S. *et al*. (1980) Oxidoreductase activities in normal rat liver, tumor-bearing rat liver, and hepatoma HC-252. *Cancer Res.*, **40**, 4677–4681.
7. Capuano,F. *et al*. (1997) Oxidative phosphorylation enzymes in normal and neoplastic cell growth. *J. Bioenerg. Biomembr.*, **29**, 379–384.
8. Capuano,F. *et al*. (1996) Oxidative phosphorylation and F(O)F(1) ATP synthase activity of human hepatocellular carcinoma. *Biochem. Mol. Biol. Int.*, **38**, 1013–1022.
9. Cuezva,J.M. *et al*. (1997) Mitochondrial biogenesis in the liver during development and oncogenesis. *J. Bioenerg. Biomembr.*, **29**, 365–377.
10. Barbour,R.L. *et al*. (1983) Adenine nucleotide transport in hepatoma mitochondria and its correlation with hepatoma growth rates and tumor size. *Cancer Res.*, **43**, 1511–1517.
11. Chen,L.B. (1988) Mitochondrial membrane potential in living cells. *Annu. Rev. Cell Biol.*, **4**, 155–181.
12. Johnson,L.V. *et al*. (1982) Decreased uptake and retention of rhodamine 123 by mitochondria in feline sarcoma virus-transformed mink cells. *Cell*, **28**, 7–14.
13. Summerhayes,I.C. *et al*. (1982) Unusual retention of rhodamine123 by mitochondria in muscle and carcinoma cells. *Proc. Natl Acad. Sci. USA*, **79**, 5292–5296.
14. Heerdt,B.G. *et al*. (2005) The intrinsic mitochondrial membrane potential of colonic carcinoma cells is linked to the probability of tumor progression. *Cancer Res.*, **65**, 9861–9867.
15. Ionov,Y. *et al*. (2000) Mutational inactivation of the proapoptotic gene BAX confers selective advantage during tumor clonal evolution. *Proc. Natl Acad. Sci. USA*, **97**, 10872–10877.
16. Johnstone,R.W. *et al*. (2002) Apoptosis: a link between cancer genetics and chemotherapy. *Cell*, **108**, 153–164.
17. Kroemer,G. (1997) The proto-oncogene Bcl-2 and its role in regulating apoptosis. *Nat. Med.*, **3**, 614–620.
18. Reed,J.C. (1997) Double identity for proteins of the Bcl-2 family. *Nature*, **387**, 773–776.
19. Ross,M.F. *et al*. (2005) Lipophilic triphenylphosphonium cations as tools in mitochondrial bioenergetics and free radical biology. *Biochemistry (Mosc.)*, **70**, 222–230.
20. Fantin,V.R. *et al*. (2006) Mitochondriotoxic compounds for cancer therapy. *Oncogene*, **25**, 4787–4797.
21. Berners-Price,S.J. *et al*. (1988) Phosphines and metal phosphine complexes: relationship of chemistry to anticancer and other biological activity. *Struct. Bond. (Berlin)*, **70**, 27–102.
22. Modica-Napolitano,J.S. *et al*. (2001) Delocalized lipophilic cations selectively target the mitochondria of carcinoma cells. *Adv. Drug Deliv. Rev.*, **49**, 63–70.
23. McKeage,M.J. *et al*. (2000) Role of lipophilicity in determining cellular uptake and antitumour activity of gold phosphine complexes. *Cancer Chemother. Pharmacol.*, **46**, 343–350.
24. Rackham,O. *et al*. (2007) A gold(I) phosphine complex selectively induces apoptosis in breast cancer cells: implications for anticancer therapeutics targeted to mitochondria. *Biochem. Pharmacol.*, **74**, 992–1002.
25. Baker,M.V. *et al*. (2006) Cationic, linear Au(I) *N*-heterocyclic carbene complexes: synthesis, structure and anti-mitochondrial activity. *Dalton Trans.*, **30**, 3708–3715.
26. Baker,M.V. *et al*. (2005) Synthesis and structural characterization of linear Au(I) *N*-heterocyclic carbene complexes: new analogues of the Au(I) phosphine drug Auranofin. *J. Organomet. Chem.*, **690**, 5625–5635.
27. Tirnitz-Parker,J.E. *et al*. (2007) Isolation, culture and immortalisation of hepatic oval cells from adult mice fed a choline-deficient, ethionine-supplemented diet. *Int. J. Biochem. Cell Biol.*, **39**, 2226–2239.
28. Brand,M.D. (1995) Measurement of mitochondrial protonmotive force. In Brown,G.C. and Cooper,C.E. (eds.) *Bioenergetics—A Practical Approach*. IRL, Oxford, pp. 39–62.
29. Brown,G.C. *et al*. (1985) Thermodynamic control of electron flux though mitochondria cytochrome bc_1 complex. *Biochem. J.*, **225**, 399–405.
30. Scott,I.D. *et al*. (1980) Energy transduction in intact synaptosomes. *Biochem. J.*, **186**, 21–33.
31. Viebahn,C.S. *et al*. (2006) Evaluation of the ''Cellscreen'' system for proliferation studies on liver progenitor cells. *Eur. J. Cell Biol.*, **85**, 1265–1274.
32. Dumble,M.L. *et al*. (2002) Generation and characterization of p53 null transformed hepatic progenitor cells: oval cells give rise to hepatocellular carcinoma. *Carcinogenesis*, **23**, 435–445.
33. Yeoh,G.C. *et al*. (1993) Transformation-induced alterations in the regulation of tyrosine aminotransferase expression in fetal rat hepatocytes: changes in hormone inducibility and the DNase-hypersensitive site. *Cancer Res.*, **53**, 515–522.
34. Galluzzi,L. *et al*. (2006) Mitochondria as therapeutic targets for cancer chemotherapy. *Oncogene*, **25**, 4812–4830.
35. Zender,L. *et al*. (2006) Identification and validation of oncogenes in liver cancer using an integrative oncogenomic approach. *Cell*, **125**, 1253–1267.
36. Pani,G. *et al*. (2004) Mitochondrial superoxide dismutase: a promising target for new anticancer therapies. *Curr. Med. Chem.*, **11**, 1299–1308.
37. Yeoh,G. *et al*. (1989) Transformation of cultured fetal rat liver cells by MDAB and phenobarbital. Morphological, biochemical and immunocytochemical characterization of cell lines. *Carcinogenesis*, **10**, 1015–1027.
38. LaCasse,E.C. *et al*. (1998) The inhibitors of apoptosis (IAPs) and their emerging role in cancer. *Oncogene*, **17**, 3247–3259.
39. Huang,J. *et al*. (2005) The Hippo signaling pathway coordinately regulates cell proliferation and apoptosis by inactivating Yorkie, the *Drosophila* homolog of YAP. *Cell*, **122**, 421–434.
40. Danovi,S.A. *et al*. (2008) Yes-associated protein (YAP) is a critical mediator of c-Jun-dependent apoptosis. *Cell Death Differ*, **15**, 217–219.
41. Yang,L.Y. *et al*. (2005) Differential expression of antioxidant enzymes in various hepatocellular carcinoma cell lines. *J. Cell. Biochem.*, **96**, 622–631.
42. Modica-Napolitano,J.S. *et al*. (2004) Mitochondrial dysfunction in cancer. *Mitochondrion*, **4**, 755–762.

43. Modica-Napolitano,J.S. *et al*. (1987) Basis for the selective cytotoxicity of rhodamine 123. *Cancer Res.*, **47**, 4361–4365.
44. Ohnami,S. *et al*. (1999) Identification of genes showing differential expression in antisense K-ras-transduced pancreatic cancer cells with suppressed tumorigenicity. *Cancer Res.*, **59**, 5565–5571.
45. Chiba,Y. *et al*. (1998) MKT-077, localized lipophilic cation: antitumor activity against human tumor xenografts serially transplanted into nude mice. *Anticancer Res.*, **18**, 1047–1052.
46. Fantin,V.R. *et al*. (2002) A novel mitochondriotoxic small molecule that selectively inhibits tumor cell growth. *Cancer Cell*, **2**, 29–42.
47. Sun,X. *et al*. (1994) AA1, a newly synthesized monovalent lipophilic cation, expresses potent *in vivo* antitumor activity. *Cancer Res.*, **54**, 1465–1471.
48. Kandela,I.K. *et al*. (2003) Effect of the lipophilic/hydrophilic character of cationic triarylmethane dyes on their selective phototoxicity toward tumor cells. *Biotech. Histochem.*, **78**, 157–169.
49. Trapp,S. *et al*. (2005) A predictive model for the selective accumulation of chemicals in tumor cells. *Eur. Biophys. J.*, **34**, 959–966.

Received February 20, 2008; revised March 20, 2008; accepted March 26, 2008